# Atomic and electronic structures of thallium-based III-V-$VI_2$ ternary chalcogenides: *Ab initio* calculations

Khang Hoang and S. D. Mahanti*
*Department of Physics and Astronomy, Michigan State University, East Lansing, Michigan 48824, USA*
(Received 12 February 2008; revised manuscript received 13 April 2008; published 13 May 2008)

The atomic and electronic structures of III-V-$VI_2$ ternary chalcogenides (III=Tl, V=Sb and Bi, and VI =Te, Se, and S) have been studied using *ab initio* electronic structure calculations. Most of these compounds are found to take rhombohedral structures as their lowest energy structures (except for $TlSbS_2$, which takes a triclinic structure), in agreement with experiments. There is a disagreement between theory and experiment in the case of $TlSbSe_2$, wherein our calculations identify a rhombohedral structure (as yet hypothetical), which has lower energy than a monoclinic one (given by experiment). Band-gap formation in these ternaries are controlled by a highly directional hybridization between the cation (Sb, Bi), anion (S, Se, Te), and Tl *p* states, and the electronic structure near the Fermi level is sensitive to the ordering on the cation sublattice.

DOI: 10.1103/PhysRevB.77.205107 PACS number(s): 71.20.Nr, 71.15.Nc, 71.28.+d

## I. INTRODUCTION

Over the last four decades, narrow band-gap semiconductors have played a dominant role in providing efficient materials for thermoelectric applications. The best known bulk thermoelectric materials are binary chalcogenides, especially doped $Bi_2Te_3$, PbTe, $Sb_2Te_3$, and their alloys.[1,2] More complex chalcogenides, e.g., ternaries and quaternaries, have also been proposed for thermoelectric applications.[1–5] Among these are Tl-based ternary chalcogenides. $TlBiTe_2$ has been suggested as a candidate material since ca. 1970s, but its use has been limited due to the fact that Tl and its compounds have to be carefully handled.[4,5] Superconductivity has also been found to occur at 0.14 K in samples of $TlBiTe_2$ with nominal carrier densities ($\sim 6\times 10^{20}$ holes/$cm^3$).[6] There has been a revival of interest in these Tl-based ternary chalcogenides for thermoelectrics inspired by promising results from several recent studies. Wölfing *et al.*[7] reported a thermoelectric figure of merit *ZT* (see below) ~1.2 at 500 K for $Tl_9BiTe_6$. This compound exhibits an extremely low thermal conductivity (0.39 W/m K at 300 K).[7] $Tl_9BiTe_6$ together with $TlBiTe_2$ is usually found in $Tl_2Te$-$Bi_2Te_3$ systems. It is reported that $TlBiTe_2$ also has a relatively low thermal conductivity, which is comparable to other state-of-the-art thermoelectric materials.[8] The Sb counterpart of this compound, $TlSbTe_2$, is also known to be a good thermoelectric (*ZT* ~0.87 at 715 K).[9]

In a thermoelectric, the figure of merit (denoted as *ZT*, where *T* is the operating temperature) depends on the thermopower *S* and the electrical conductivity $\sigma$ through the relation $ZT=\sigma S^2T/\kappa$, where $\kappa$ is the thermal conductivity (including both the electronic and lattice contributions) of the material. Clearly, large values of *ZT* require large values of *S* and $\sigma$, both of which sensitively depend on the nature of the electronic states near the band gap.[10] Thus, it is important to understand the nature of these states (i.e., the formation of band gaps) in different Tl-based ternaries and how they change when one modifies their atomic structures and/or replaces one constituent element by another. Based on this understanding, one can explain, predict, and optimize the properties of the materials and suggest new materials for better performance.

Although $TlSbQ_2$ and $TlBiQ_2$ ($Q$=Te, Se, and S) have been experimentally studied, to the best of our knowledge, there are very few, if any, theoretical investigations on the atomic and electronic structures of these Tl-based ternaries except for some earlier studies of $TlSbSe_2$ by Ren *et al.*[11] and of $TlSbS_2$ by Lefebvre *et al.*[12,13] that used tight-binding approximation. In this paper, we present our extensive studies of the structural properties, energetics, and electronic structure of Tl-based III-V-$VI_2$ ternary chalcogenides using *ab initio* electronic structure calculations. The arrangements of this paper are as follows: In Sec. II, we present different ordered structures of Tl-based III-V-$VI_2$ ternary chalcogenides (both experimental and hypothetical) and their energetics. The interplay between atomic and electronic structures and the band-gap formation in $TlSbQ_2$ and $TlBiQ_2$ will be discussed in Sec. III. We will conclude our paper with a summary in Sec. IV.

## II. STRUCTURE AND ENERGETICS

$TlSbTe_2$ and $TlBiTe_2$ were first reported to have disordered NaCl-type structures.[14] Hockings and White[15] later found that these two Tl-based tellurides have ordered structures, which are isostructural with the intermediate phases of $AgBiSe_2$ and $AgBiS_2$.[16] These structures are formed by the ordering of the cations in the layers perpendicular to one of the cubic [111] directions, which are denoted as AF-II (see below).[17,18] Recent studies of $TlBiTe_2$ by Chrissafis *et al.*[19] showed a solid-solid phase transformation from rhombohedral (low-temperature phase) to cubic (high-temperature phase) symmetry. The other two Bi compounds, $TlBiSe_2$ and $TlBiS_2$, were also found to possess a rhombohedral structure.[20,21]

The literature on the crystal structure of $TlSbSe_2$ is somewhat controversial. Botgros *et al.*[22] reported an orthorhombic structure with $a$=4.20 Å, $b$=9.0 Å, and $c$=24.0 Å, whereas Wacker *et al.*[23] found a monoclinic structure at room

 

TABLE I. Structural properties and the total energies ($E$) of different ordered structures of $TlSbQ_2$ and $TlBiQ_2$ ($Q$=Te, Se, and S) and their differences ($\Delta E$). The primitive cells of AF-II and AF-IIb structures are, respectively, rhombohedral ($R\bar{3}m$, 4 atoms/cell) and face-centered cubic (fcc, $F\bar{3}dm$, 16 atoms/cell). MCN is monoclinic ($P2_1$, 16 atoms/cell) and TCN is triclinic ($P\bar{1}$, 16 atoms/cell). The coordinates for MCN and TCN are taken from experiments.

| Structure | | Lattice parameters (Å) | | Energy (eV/f.u.) | |
|---|---|---|---|---|---|
| | | Calc. | Expt. | $E$ | $\Delta E$ |
| $TlSbTe_2$ | AF-II | $a$=4.438, $c$=23.371 | $a$=4.425, $c$=23.303 [a] | −13.8979 | 0 |
| | AF-IIb | $a$=12.880 | | −13.8796 | 0.0183 |
| $TlSbSe_2$ | AF-II | $a$=4.178, $c$=22.408 | | −14.9271 | 0 |
| | AF-IIb | $a$=12.180 | | −14.8773 | 0.0498 |
| | MCN | $a$=9.263, $b$=4.154, $c$=13.236 | $a$=9.137(1), $b$=4.097(1), $c$=12.765(2) | −14.8598 | 0.0673 |
| | | $\beta$=111.99 | $\beta$=111.75(1) [b] | | |
| $TlSbS_2$ | AF-II | $a$=4.013, $c$=21.752 | | −15.9962 | 0.0879 |
| | AF-IIb | $a$=11.750 | | −15.9189 | 0.1652 |
| | TCN | $a$=6.236, $b$=6.273, $c$=11.879 | $a$=6.123(6), $b$=6.293(10), $c$=11.838(13) | −16.0841 | 0 |
| | | $\alpha$=101.70, $\beta$=96.94, $\gamma$=104.59 | $\alpha$=101.34(7), $\beta$=98.39(5), $\gamma$=103.21(19) [c] | | |
| $TlBiTe_2$ | AF-II | $a$=4.534, $c$=23.512 | $a$=4.527, $c$=22.118 [d] | −14.4087 | 0 |
| | AF-IIb | $a$=13.075 | | −14.3998 | 0.0089 |
| $TlBiSe_2$ | AF-II | $a$=4.264, $c$=22.478 | $a$=4.24, $c$=22.33 [e] | −15.4537 | 0 |
| | AF-IIb | $a$=12.360 | | −15.4329 | 0.0208 |
| $TlBiS_2$ | AF-II | $a$=4.096, $c$=22.845 | $a$=4.104, $c$=21.93 [f] | −16.4990 | 0 |
| | AF-IIb | $a$=11.920 | | −16.4617 | 0.0373 |

[a]Rhombohedral $R\bar{3}m$ (Ref. 15).
[b]Monoclinic $P2_1$ (Ref. 23).
[c]Triclinic $P\bar{1}$ (Ref. 24).
[d]Rhombohedral $R\bar{3}m$ (Ref. 15).
[e]Rhombohedral $R\bar{3}m$ (Ref. 20).
[f]Rhombohedral $R\bar{3}m$ (Ref. 26).

temperature. On the other hand, $TlSbS_2$ was found to have a triclinic structure.[24] The monoclinic structure of $TlSbSe_2$ and the triclinic structure of $TlSbS_2$ will be denoted as MCN and TCN, respectively. In Table I, we give a summary of the experimental structures and the lattice parameters of $TlSbQ_2$ and $TlBiQ_2$.

### A. Different ordered structures for the electronic structure calculations of Tl-based III-V-$VII_2$ ternaries

Due to the existence of the rhombohedral symmetry in the majority of the Tl-based compounds, AF-II (space group $R\bar{3}m$) (Ref. 17) with alternating Tl, $Q$ (group VII atoms), and Sb (or Bi) planes normal to the [111] direction [see Fig. 1(a)] is selected for the present studies. Another related structure, AF-IIb (space group $F\bar{3}dm$) with alternating Tl-Sb(Bi) and $Q$ planes normal to the [111] direction, is also selected because of its closeness in energy with AF-II as seen in many I-V-$VII_2$ ternaries,[17,25] although it is, as yet, a hypothetical structure. AF-IIb (not shown) can be obtained from AF-II by rotating the second and the fourth layers of AF-II by 90° around the vertical axis. This structure has a face-centered cubic (fcc) symmetry. The possibility of having a transformation between AF-II and AF-IIb in these chalcogenides will be examined later. The MCN and TCN structures for $TlSbSe_2$ and $TlSbS_2$ [Figs. 1(b) and 1(c)], respectively, which are available in literature,[23,24] are also analyzed. These two structures are layered structures; however, the local coordination of the atoms in these two structures is very different (from each other and from the AF-II and AF-IIb structures). In the monoclinic $TlSbSe_2$, which has (double) layers parallel to the (001) plane [Fig. 1(b)], Sb and Tl atoms have five bonds to Se atoms of 2.576–3.025 Å (Sb-Se) or 3.097–3.289 Å (Tl-Se).[23] The shortest distance between the two double layers is 3.625 Å between the Tl atoms from one double layer to the Tl atoms in the other. In the TCN $TlSbS_2$ with layers parallel to the (010) plane [Fig. 1(c)], the Sb atoms have four bonds to S atoms of 2.41–2.96 Å.[24] The shortest distance between the layers in the TCN structure is ~3.50 Å.

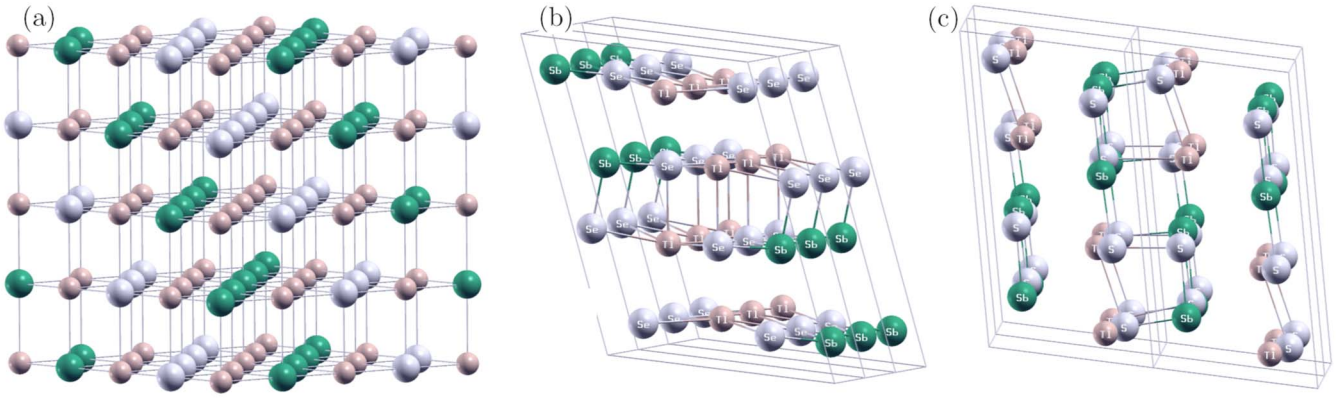


FIG. 1. (Color online) Different ordered structures of $TlSbQ_2$ and $TlBiQ_2$: (a) AF-II structure with alternating Tl, $Q$, and Sb (or Bi) planes normal to the [111] direction; (b) MCN structure of $TlSbSe_2$; and (c) TCN structure of $TlSbS_2$ with the coordinates taken from experiments (see the text). AF-IIb with alternating Tl-Sb(Bi) and $Q$ planes normal to the [111] direction (not shown) can be obtained from AF-II by rotating the second and the fourth layers of AF-II by 90° around the vertical axis. The large balls are for Tl and Sb(Bi), and the small balls are for $Q$.

### B. Computational details

Structural optimization, total energy, and electronic structure calculations were performed within the density functional theory (DFT) formalism using the generalized-gradient approximation[27] (GGA) and the projector-augmented wave (PAW)[28] method as implemented in the VASP code.[29] We treated the outmost $s$ and $p$ electrons of the constituent atoms as valence electrons and the rest as cores (i.e., by using the standard PAW potentials in the VASP database). Scalar relativistic effects (mass velocity and Darwin terms) and spin-orbit interaction (SOI) were included except in ionic optimization, wherein only scalar relativistic effects were taken into account since the inclusion of SOI was found not to have a significant influence.[30] Each calculation begins with the ionic optimization of a chosen structure; the relaxed structure was then used to calculate the energy, single-particle electronic density of states (DOS), and band structure.

### C. Calculated structural parameters

In Table I, we summarize the structural parameters of AF-II, AF-IIb, MCN, and TCN obtained after structural optimization. The lattice parameters of the rhombohedral primitive cells are given in the hexagonal cell representation. The results for AF-II are in excellent agreement with experiments (within ~1%–3% due to the overestimation of DFT-GGA; see, e.g., Ref. 31). MCN and TCN slightly change their lattice parameters after structural optimization due to the rearrangement of the atoms in these systems, although their bond lengths do not change much (the deviation from those of experiments is less than 1%).

### D. Energetics

The rhombohedral AF-II is found to be the lowest energy structure in all the compounds except in $TlSbS_2$ (see Table I). This is consistent with experiments wherein many Tl-based ternary chalcogenides have been found to possess a rhombohedral structure. We also find TCN to be the lowest energy structure of $TlSbS_2$, which is in agreement with experiment.

MCN (as seen in experiments) is not the lowest energy structure of $TlSbSe_2$. It is higher in energy than AF-II by ~70 meV, and even higher than the fcc AF-IIb (by ~20 meV). This is quite puzzling since DFT calculations give the lowest energy structure in the rest of the systems. One, therefore, should reanalyze $TlSbSe_2$ samples to see if the rhombohedral AF-II can give a better fit to the x-ray diffraction data. One should also examine to see if there is a transformation to a rhombohedral phase at a lower temperature. In $TlSbS_2$, TCN has much lower energy than AF-II and AF-IIb (by ~88 and 165 meV, respectively) which suggests that the TCN is energetically extremely stable. In $TlBiTe_2$, on the other hand, AF-II and AF-IIb are very close in energy (~9 meV different). Experimentally, it was observed that the phase transformation of $TlBiTe_2$ was a "multiple-step displacive-martensitic-type" transformation.[19] Based on our calculations, one may expect to see the system, if it is annealed from a cubic NaCl type, pass through the fcc AF-IIb before going to the rhombohedral AF-II lattice.

To summarize the structural aspects of the Tl-based ternary chalcogenides, the rhombohedral AF-II (for $TlSbTe_2$ and $TlBiQ_2$) and the TCN (for $TlSbS_2$) are found to be the lowest energy structures, consistent with experiments. The lowest energy structure for $TlSbSe_2$ is, however, AF-II, not the experimental MCN.

## III. ELECTRONIC STRUCTURE

### A. Electronic structure of $TlSbQ_2$

In Figs. 2(a) and 2(b), we show the total DOS of $TlSbTe_2$ and $TlSbSe_2$ in different ordered structures. There is very little difference between AF-II and AF-IIb in the DOS of $TlSbTe_2$ near the Fermi level ($\epsilon_F$) except for a small transfer of electronic states ranging from ~−0.4 to −0.2 eV to lower energies in going from AF-IIb to AF-II. The transfer of these states results in lowering the energy of AF-II (by ~18 meV/f.u., see Table I). From the total DOS, we find

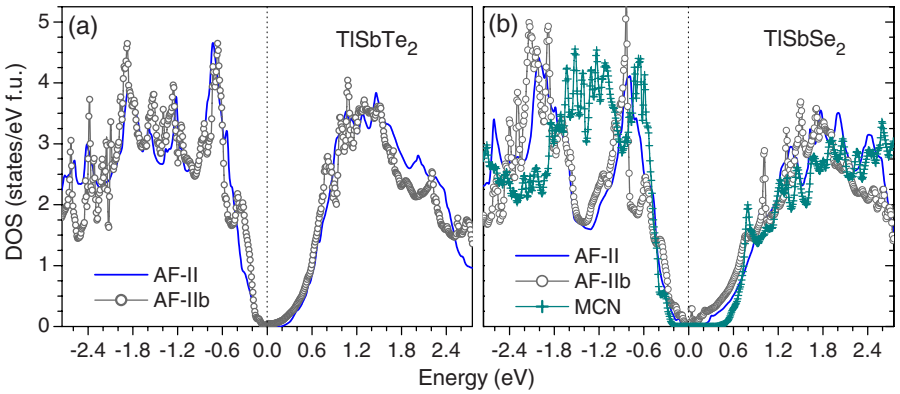


FIG. 2. (Color online) DOSs of $TlSbQ_2$ ($Q$=Te,Se) in the AF-II, AF-IIb, and MCN structures. The DOSs of $TlSbSe_2$ in AF-II and MCN are shifted by ~0.080 and 0.166 eV, respectively, so that the bottom of the valence bands match. The Fermi level is set at the highest occupied state (for AF-IIb in the case of $TlSbSe_2$).

that the AF-IIb gives $TlSbTe_2$ a pseudogap (with DOS ~ 0 at $\epsilon_F$), whereas the rhombohedral AF-II gives a band gap of ~0.2 eV.

As regards $TlSbSe_2$, the MCN gives a band gap of ~0.5 eV as compared to ~0.1 eV (for AF-II) and ~0 eV (for AF-IIb). The band-gap value of the monoclinic $TlSbSe_2$ is in good agreement with that obtained in tight-binding calculations by Ren *et al.*[11] (which gave an indirect band gap of 0.58 eV) and is comparable to the experimental value of ~0.82 eV.[32] However, as we have mentioned, MCN is not the structure that gives $TlSbSe_2$ the lowest energy at zero temperature (see Table I). This can be understood in terms of the obtained DOS [see Fig. 2(b)]. Although there is a transfer of electronic states near the valence band-top DOS (ranging from −0.4 eV to 0 eV) to lower energies in going from AF-II and AF-IIb to MCN, there is a much larger transfer of states from lower to higher energies in the region ranging from ~−2.5 to −0.4 eV. This results in a higher energy for MCN. It is also noted that there are significant differences in the electronic structure in MCN compared to that in AF-II and AF-IIb [see Fig. 2(b)].

For $TlSbS_2$, the higher energy AF-II structure gives a band gap of ~0.06 eV, whereas the lower energy TCN structure gives a much larger band gap (~1.3 eV); see the DOS in Fig. 3(a). The latter value is comparable to that of 1.907 eV (at 2 K) obtained by Rouquette *et al.*[33] in optical absorption measurements. In order to see the nature of the electronic states in the band-gap region, the partial density if states (PDOS) associated with the $s$ and $p$ orbitals of Tl, Sb, and S for both AF-II and TCN structures are plotted in Figs. 3(b) and 3(c), respectively. The PDOS analysis shows that the valence-band top is predominantly S $p$, whereas the conduction-band bottom is predominantly Tl $p$ and Sb $p$ [Figs. 3(b) and 3(c)]. The $p$ states of Tl, therefore, play an important role in the formation of band gap in the Tl-based III-V-$VI_2$ ternary chalcogenides, which is different from the I-V-$VI_2$ systems (I=Na, Ag, and Cu), wherein it is the $s$ state of the monovalent atom.[17,25] The above analysis also suggests that Tl behaves like $Tl^+$ (monovalent) in these ternaries.

We now discuss how the band structures change as one keeps the cations fixed and change the divalent anion, keeping the atomic structure fixed. One would expect the degree of splitting between the valence and the conduction bands to increase as one goes from Te → Se → S. However, this is not the case due to strong spin-orbit effects and hybridization. The band structures of $TlSbQ_2$ obtained in calculations with and without SOI are shown in Figs. 4(a)–4(d). These calculations made use of the rhombohedral AF-II structure, although AF-II is not the lowest energy structure of $TlSbS_2$.

As seen in Figs. 4(a)–4(d), SOI has strong effects in the telluride. The band gap of $TlSbTe_2$ (~0.2 eV, a direct gap at the Γ point of the rhombohedral BZ) is a spin-orbit-induced gap (the band gap opens up through SOI). In the selenide, calculation leads to a spin-orbit-induced gap near the Γ point and along the Γ-$L$ direction of the rhombohedral BZ [see Fig. 4(b)]. This gap and a similar one near Γ and along the Γ-$X$ direction (not shown), which are hybridization-induced gaps (caused by the crossover between the valence band top and the conduction band bottom at and near the Γ point), create a multipeak structure near the top of the valence band and near the bottom of the conduction band. However, the smallest gap of $TlSbSe_2$ in the AF-II structure is an indirect

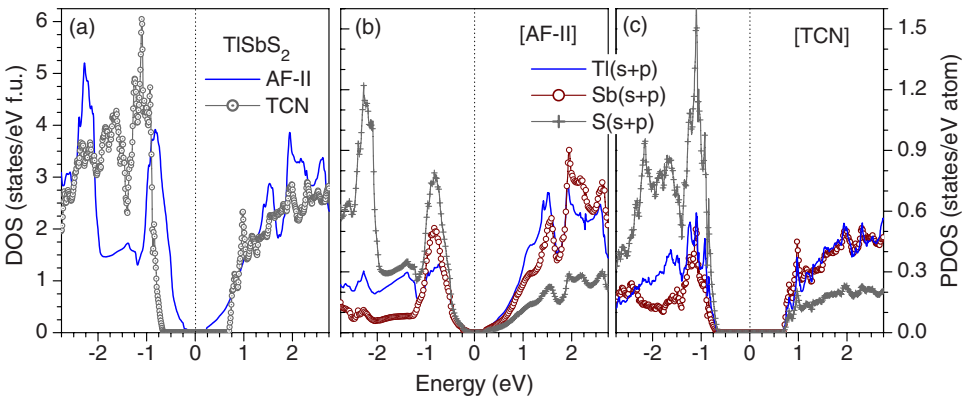


FIG. 3. (Color online) DOSs and PDOSs of $TlSbS_2$ in the AF-II, AF-IIb, and TCN structures. The DOS and PDOS in TCN are shifted by ~0.644 eV so that the bottom of the valence bands match. The Fermi level is set at the highest occupied states for AF-II.

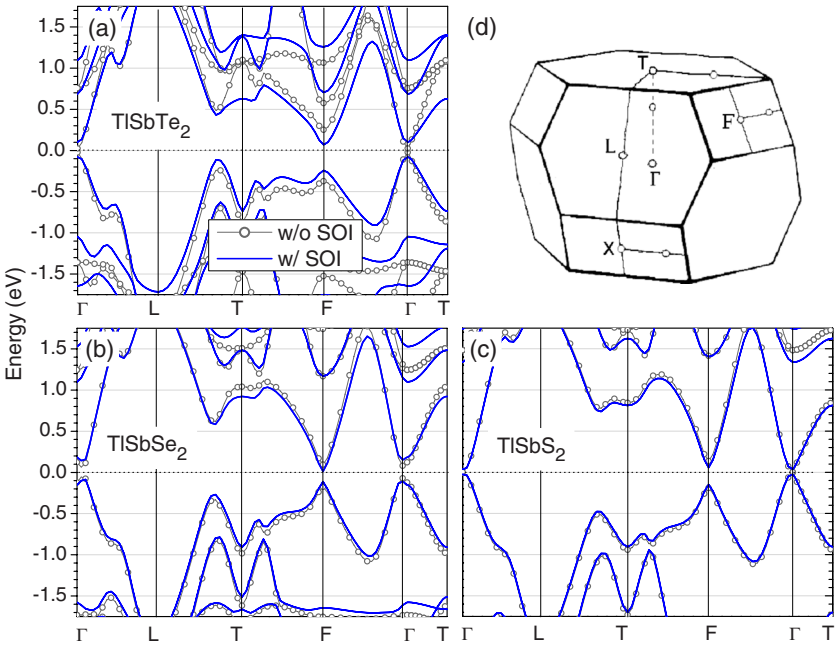


FIG. 4. (Color online) [(a)–(c)] Band structures of $TlSbQ_2$ ($Q$ =Te, Se, and S) along the high symmetry directions of the Brillouin zone of the (d) rhombohedral AF-II structure. The results were obtained in calculations with (solid curves) and without (circled curves) SOI.

gap (of ~0.1 eV) between the maximum near Γ (and along the Γ-$L$ direction) and the minimum at the F (or $X$) point. In the sulfide, SOI has very small effect on the band structure near $\epsilon_F$ as one would expect [see Fig. 4(c)]. Our calculations give a direct band gap of ~0.06 eV (at Γ) for $TlSbS_2$ in the AF-II structure. The band gap (in the AF-II structure), therefore, decreases in going from the telluride to selenide to sulfide.

In $TlSbQ_2$, the valence band top and conduction band bottom are quite symmetric through the Fermi level except along the $L$-$T$ and $T$-$F$ directions, where there is band asymmetry and the maxima in the valence band are closer to $\epsilon_F$ (the zero of energy) than the minima in the conduction band. In the case of $TlSbTe_2$, the peak (at ~−0.15 eV) along the $L$-$T$ direction [see Fig. 4(a)] can contribute to the transport, which results in a large positive thermopower as seen in experiments, ~220$\mu$V/K at 630 K.[9] The energy of this peak goes away from $\epsilon_F$ in going from telluride to selenide to sulfide.

### B. Electronic structure of $TlBiQ_2$

SOI effects should be stronger in $TlBiQ_2$ compounds since Bi is heavier than Sb. This can be seen in Figs. 5(a)–5(c), wherein the band structures of $TlBiQ_2$ obtained in calculations with and without SOI in the rhombohedral AF-II structure are shown. The SOI significantly changes the band structure of $TlBiTe_2$ since all the three elements Tl, Bi, and

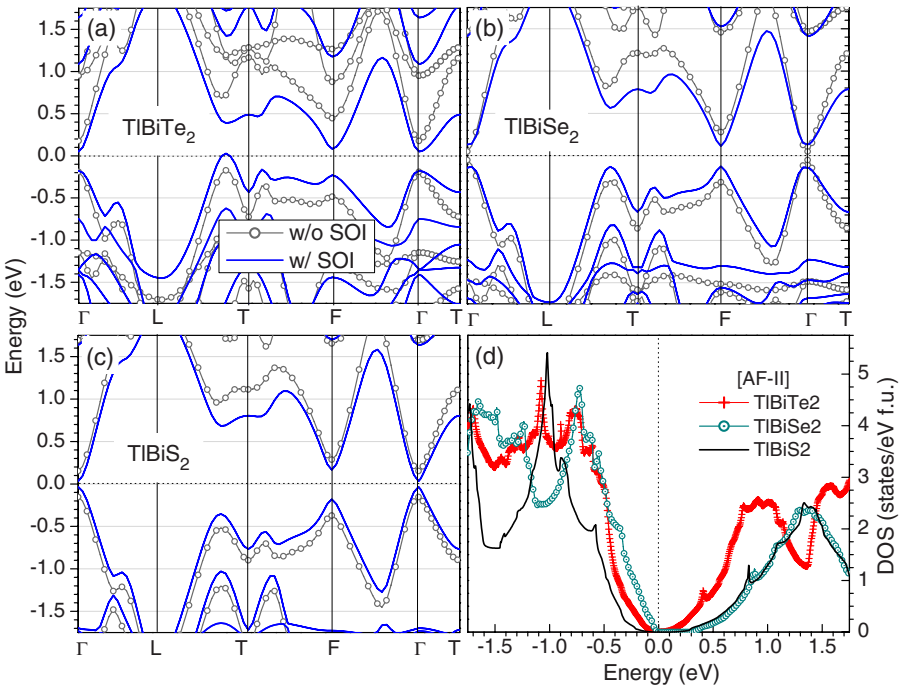


FIG. 5. (Color online) [(a)–(c)] Band structures and (d) DOSs of $TlBiQ_2$ ($Q$=Te, Se, and S) along the high symmetry directions of the Brillouin zone of the rhombohedral AF-II structure. The band structures were obtained in calculations with (solid curves) and without (circled curves) SOI, whereas all of the DOSs presented in (d) were obtained in calculations with SOI. The Fermi level is set at the highest occupied states in (d).

Te are heavy elements. From the total DOS [Fig. 5(d)], $TlBiQ_2$ is found to have a band gap of ~0.01 eV (indirect) for $Q$=Te, ~0.25 eV (direct, at the $X$ point) for $Q$=Se, or 0.07 eV (direct, at the $\Gamma$ point) for $Q$=S. In the case of $TlBiTe_2$, the conduction band minimum is at $\Gamma$, whereas the valence band maximum is near the $T$ point and along the $T$-$L$ line [see Fig. 5(a)]. Experimentally, it is reported that $TlBiS_2$ and $TlBiSe_2$ have band gaps of 0.4 and 0.28 eV, respectively,[20] whereas $TlBiTe_2$ has a band gap of 0.11 eV.[34] Although the DFT problem of underestimating band gaps[31] is consistent with what we find in the sulphide and the telluride, the selenide situation is puzzling. A possible reason may be due to the complex nature of the gap formation in these ternary compounds resulting from the interplay of hybridization and spin-orbit interaction.

As it is in the $TlSbQ_2$ compounds, there is also a band asymmetry between the valence band top and the conduction band bottom along the $L$-$T$ and $T$-$F$ directions in $TlBiQ_2$ band structures that makes them good for $p$-type thermoelectric materials. Experimentally, it is reported that $n$-type $TlBiTe_2$ has $ZT$=0.15 at 760 K,[8] which is much smaller than $p$-type $TlSbTe_2$ which gives $ZT$=0.87 at 715 K.[9] The smaller $ZT$ value is due to the small (and negative) thermopower in $TlBiTe_2$ (~−70 $\mu$V/K on average).[8] Based on the calculated band structure, we suggest that $TlBiTe_2$ should be made $p$ type to take advantage of the band asymmetry, especially the flat band and multipeak features near the $T$ point and $F$ point [see Fig. 5(a)]. This goal, however, may not be easy to achieve in practice since it has been reported that $TlBiTe_2$ consistently shows $n$-type conductivity,[6,8,35] whereas $TlSbTe_2$ shows $p$-type conductivity.[9] The reason for this may come from the defect complexes and/or secondary phases that are present in the samples but are different in different compounds. More theoretical and experimental studies are needed to understand this matter and also to learn how to control the conductivity of the systems.

## IV. SUMMARY

In summary, we have carried out detailed studies of the structural properties, energetics, and electronic structure of Tl-based III-V-$VII_2$ ternary chalcogenides ($V$=Sb,Bi and VII=S, Se, and Te). The total energy calculations identify the rhombohedral AF-II structure as the lowest energy structure in most of the $TlSbQ_2$ and $TlBiQ_2$ compounds except in $TlSbS_2$, for which the theoretical calculations give the triclinic structure (in agreement with experiments). There is, however, disagreement between theory and experiment in the case of $TlSbSe_2$, for which experiments give a monoclinic structure, whereas our calculations identify the rhombohedral AF-II as the lowest energy structure. In view of this, we suggest experimentally reexamining the structure and/or carrying out further studies to see if there is phase transition at low temperature.

The highly directional hybridization between the trivalent cation (Sb and Bi), anion (S, Se, and Te), and Tl $p$ states is found to play an important role in the band-gap formation of the ternary chalcogenides. The ordering on the cation sublattice, therefore, has a huge impact on the electronic structure of Tl-based III-V-$VII_2$ in the neighborhood of the Fermi energy. The physics of gap formation is more complicated in Tl-based III-V-$VI_2$ than in I-V-$VII_2$ (I=Na, Ag, and Cu) ternary chalcogenides because of the strong spin-orbit effects, hybridization, and the participation of the directional and degenerate Tl $p$ bands. Spin-orbit interaction can either reduce or increase the band gap, depending on the specific system and the specific symmetry point in the Brillouin zone. Based on the calculated band structures, we have identified $TlSbTe_2$, $TlSbSe_2$, $TlBiTe_2$, and $TlBiSe_2$ (all in the rhombohedral structure) as promising $p$-type thermoelectrics.

## ACKNOWLEDGMENTS

This work was partially supported by MURI Grant No. N00014-03-10789 from the Office of Naval Research. Calculations were partly performed at the High Performance Computing Center of Michigan State University.

*Corresponding author; mahanti@pa.msu.edu

[1] C. Wood, Rep. Prog. Phys. **51**, 459 (1988).
[2] G. D. Mahan, Solid State Phys. **51**, 81 (1998).
[3] K.-F. Hsu, S. Loo, F. Guo, W. Chen, J. S. Dyck, C. Uher, T. Hogan, E. K. Polychroniadis, and M. G. Kanatzidis, Science **303**, 818 (2004).
[4] L. G. Voinova, V. A. Bazakutsa, S. A. Dembovskii, L. G. Lisovskii, E. P. Sokol, and C. T. Kantser, Izv. Vyssh. Uchebn. Zaved. Fiz. **5**, 154 (1971) (in Russian).
[5] A. S. Tsytko, S. A. Dembovskii, I. I. Ezhik, and V. A. Bazakutsa, Izv. Vyssh. Uchebn. Zaved. Fiz. **12**, 154 (1969) (in Russian).
[6] R. A. Hein and E. M. Swiggard, Phys. Rev. Lett. **24**, 53 (1970).
[7] B. Wölfing, C. Kloc, J. Teubner, and E. Bucher, Phys. Rev. Lett. **86**, 4350 (2001).
[8] K. Kurosaki, A. Kosuga, and S. Yamanaka, J. Alloys Compd. **351**, 279 (2003).
[9] K. Kurosaki, H. Uneda, H. Muta, and S. Yamanaka, J. Alloys Compd. **376**, 43 (2004).
[10] G. D. Mahan and J. O. Sofo, Proc. Natl. Acad. Sci. U.S.A. **93**, 7436 (1996).
[11] J. Ren, M.-H. Whangbo, H. Bengel, H.-J. Cantow, and S. N. Magonov, Chem. Mater. **5**, 1018 (1993).
[12] I. Lefebvre, M. Lannoo, G. Allan, A. Ibanez, J. Fourcade, J. C. Jumas, and E. Beaurepaire, Phys. Rev. Lett. **59**, 2471 (1987).
[13] I. Lefebvre, M. Lannoo, G. Allan, and L. Martinage, Phys. Rev. B **38**, 8593 (1988).
[14] S. A. Semiletov and L. I. Man, Kristallografiya **4**, 414 (1959).
[15] E. F. Hockings and J. G. White, Acta Crystallogr. **14**, 328 (1961).
[16] S. Geller and J. H. Wernick, Acta Crystallogr. **12**, 46 (1959).
[17] K. Hoang, S. D. Mahanti, J. R. Salvador, and M. G. Kanatzidis, Phys. Rev. Lett. **99**, 156403 (2007).

[18] We describe different types of ordering on the cation sublattice by using the standard nomenclature of antiferromagnetic orderings; see more details in Ref. 17.
[19] K. Chrissafis, E. S. Vinga, K. M. Paraskevopoulos, and E. K. Polychroniadis, Phys. Status Solidi A **196**, 515 (2003).
[20] O. Madelung, *Semiconductors: Data Handbook*, 3rd ed. (Spinger, Berlin, 2004), and references therein.
[21] N. B. Brandt, D. V. Gitsu, N. S. Popovich, V. I. Sidorov, and S. M. Chudinov, Sov. Phys. Semicond. **8**, 390 (1974).
[22] I. V. Botgros, K. R. Zbigli, A. V. Stanchu, G. I. Stepanov, A. G. Cheban, and G. D. Chumak, Inorg. Mater. **11**, 1675 (1975).
[23] K. Wacker, M. Salk, G. Decker-Schultheiss, and E. Keller, Z. Anorg. Allg. Chem. **606**, 51 (1991).
[24] P. N. Rey, J. C. Jumas, J. Olivier-Fourcade, and E. Philippot, Acta Crystallogr., Sect. C: Cryst. Struct. Commun. **39**, 971 (1983).
[25] K. Hoang, S. D. Mahanti, and M. G. Kanatzidis, (unpublished).
[26] M. Özer, K. M. Paraskevopoulos, A. N. Anagnostopoulos, S. Kokou, and E. K. Polychroniadis, Semicond. Sci. Technol. **11**, 1405 (1996).
[27] J. P. Perdew, K. Burke, and M. Ernzerhof, Phys. Rev. Lett. **77**, 3865 (1996).
[28] P. E. Blöchl, Phys. Rev. B **50**, 17953 (1994); G. Kresse and D. Joubert, *ibid.* **59**, 1758 (1999).
[29] G. Kresse and J. Hafner, Phys. Rev. B **47**, 558 (1993); G. Kresse and J. Hafner, *ibid.* **49**, 14251 (1994); G. Kresse and J. Furthmüller, *ibid.* **54**, 11169 (1996); G. Kresse and J. Furthmüller, Comput. Mater. Sci. **6**, 15 (1996).
[30] L. E. Ramos, L. K. Teles, L. M. R. Scolfaro, J. L. P. Castineira, A. L. Rosa, and J. R. Leite, Phys. Rev. B **63**, 165210 (2001).
[31] W. G. Aulber, L. Jonsson, and J. W. Wilkins, Solid State Phys. **54**, 1 (2000).
[32] J. Banys, J. Grigas, V. Valiukenas, and K. Wacker, Solid State Commun. **82**, 633 (1992); D. V. Gitsu, I. N. Grincheshen, V. F. Krasovsky, and N. S. Popovich, Fiz. Tekh. Poluprovodn. (S.-Peterburg) **22**, 152 (1988).
[33] P. Rouquette, J. Allegre, B. Gil, J. Camassel, H. Mathieu, A. Ibanez, and J. C. Jumas, Phys. Rev. B **33**, 4114 (1986).
[34] O. Valassiades, E. K. Polychroniadis, J. Stoemenos, and N. A. Economou, Phys. Status Solidi A **65**, 215 (1981).
[35] J. D. Jensen, J. R. Burke, D. W. Ernst, and R. S. Allgaier, Phys. Rev. B **6**, 319 (1972).